# Testing quantum adiabaticity with quench echo

H. T. Quan and W. H. Zurek\*

Theoretical Division, MS B213, Los Alamos National Laboratory, Los Alamos, NM, 87545, U.S.A.

Adiabaticity of quantum evolution is important in many settings; one example is the adiabatic quantum computation (AQC). Nevertheless, to date, there is no effective method available for testing the adiabaticity of the evolution for the case where the eigenenergies of the driven Hamiltonian are not known. We propose a simple method for checking adiabaticity of a quantum process for an arbitrary quantum system. We further propose an operational method for finding more efficient protocols that approximate adiabaticity, and suggest a "uniformly adiabatic" quench scheme based on the Kibble-Zurek mechanism for the case where the initial and the final Hamiltonians are given. This method should help in implementing AQC and other tasks where preserving the system in the ground state of a time-dependent Hamiltonian is desired.

PACS numbers: 03.65.Aa, 03.65.Vf, 03.67.-a, 05.30.Rt

# I. INTRODUCTION

In a quantum quench process, when the Hamiltonian of a quantum system is driven from  $H_0$  to  $H_1$ , interstate excitations of the system usually occur, owing to the non-commutativity of the Hamiltonians at different moments. However, when the quench process is slow enough, the interstate excitations will be suppressed. According to the quantum adiabatic theorem [1], when the condition for quantum adiabatic approximation  $\left\langle \Phi_{\rm ground}(t) | \frac{dH(t)}{dt} | \Phi_{\rm excited}(t) \right\rangle \ll \Delta(t)^2$  is satisfied, the system will remain in the ground state – its evolution will be adiabatic – except for some special situations [2]. Here H(t) is the changing Hamiltonian, and  $\Delta(t)$  is the minimal energy gap between the ground state  $|\Phi_{\rm ground}(t)\rangle$  and the first excited state  $|\Phi_{\rm excited}(t)\rangle$  of H(t).

In order to ensure that a quantum system evolves adiabatically, one usually needs to find the energy spectrum (or at least the smallest energy gap  $\Delta$ ) of the driven Hamiltonian. One can then use the quantum adiabatic theorem to choose a proper time scale, so that the conditions for quantum adiabatic approximation are satisfied and the evolution remains adiabatic. Nevertheless, in practice, neither eigenenergies nor eigenstates of a complex quantum many-body system are easy to obtain. This is often the case in implementing the adiabatic quantum computation (AQC) [6] as well as quantum annealing [7, 8]. Hence, one does not have the ingredients to use quantum adiabatic theorem. One cannot count on the direct comparison between the final state and the instantaneous ground state of the final Hamiltonian, either. Thus, it would be useful to find a reliable method for evaluating the adiabaticity of an evolution under an arbitrary Hamiltonian, especially when one has no idea about the eigenstates and/or eigenenergies of the system (except at the initial moment).

The quench echo method we propose here is one solution to the above problem. It will allow one to evaluate unambiguously the adiabaticity of a process. What is more, it can help one find the efficient "uniformly adiabatic" quench path in the parameter space of the Hamiltonian. Such ideas may have applications in the implementation of AQC [6]. This paper is organized as follows: In section II, we introduce the quench echo method and briefly explain its underlying physics. In section III, we use a simple model to demonstrate main ideas of the general theory. In Section IV, we propose a uniformly adiabatic scheme that is based on the application of the Kibble-Zurek mechanism (KZM) to quantum phase transitions. In Section V we give discussions and conclusions.

## II. QUENCH ECHO

Consider a system described by the Hamiltonian H(g(t)), where g(t) is a time-dependent parameter. The system is initially prepared in the ground state of H(g(t=0)). The system evolves under the influence of the driven Hamiltonian, which changes from H(g(t=0)) to H(g(t=T)). Our aim is to test the adiabaticity of this evolution, but we know nothing about the eigenenergies and eigenstates of the time-dependent Hamiltonian except at t=0. Hence we cannot count on the comparison between the evolving state and the instantaneous ground state. Neither can we use the adiabatic theorem. Nevertheless, we can apply a backward "echo" quench following the initial quench (from t=0 to t=T). That is, one extends the evolution from

<sup>\*</sup>Electronic address: whzurek@gmail.com; URL: http://public.lanl.gov/whz/

t = T to t = 2T [9]:

$$H(g(t)) = \begin{cases} H(g(t)), (0 < t < T) \\ H(g(2T - t)), (T < t < 2T) \end{cases}$$
 (1)

The final Hamiltonian is identical to the initial Hamiltonian  $H(g(t=2T)) \equiv H(g(t=0))$ . Hence, we can use the fidelity of the initial state, e.g., the ground state of H(g(t=0)) and the final evolving state as a criterion for the adiabaticity of the evolution.

$$F = \left| \langle GS | \hat{T} e^{-i \int_T^{2T} H(g(2T-t)) dt} \hat{T} e^{-i \int_0^T H(g(t)) dt} | GS \rangle \right|^2, \tag{2}$$

where T is the time-ordered operator and  $|GS\rangle$  is the ground state of H(g(t=0)). When the fidelity F is greater than a threshold value close to unity, (e.g., 0.999, the error tolerance is 0.001), the whole process (0 < t < 2T) is adiabatic. This implies that the forward quench process (0 < t < T) is adiabatic. The underlying mechanism for this "quench echo" method is straightforward: Except for the eigenstate of the Hamiltonian at the initial moment H(g(t=0)), we do not have any information about its eigenstates at other moments. Hence, we can only quench the Hamiltonian back, so that it goes back to its initial H(q(t=0)), and we can measure the final state (and compare it with the initial state). The quench echo protocol (Eq. (1)) ensures that the excitation probabilities in the forward quench process and those in the backward quench process are similar (but not identical; see Refs. [11, 12]). As a result, when the forward process is adiabatic (no excitations), so is the backward quench process. Otherwise both the forward and the backward processes are nonadiabatic, and the phase accumulated between transitions (known as the Stückelberg phase) may result in constructive or destructive interference [5, 13]. Usually the excitations in the forward and the backward processes cannot cancel each other out (but see Ref. [5]). Hence, through this quench echo method, without knowing about the eigenenergies and eigenstates, one is able to evaluate the adiabaticity of an arbitrary evolution in most cases. Nevertheless, in some special cases (e. g., impulse evolution, which is so fast that the state of the system is frozen) the final fidelity is equal to unity, but the process may not be adiabatic. A solution to this problem is to let the system evolve freely for some time before the backward quench. We will discuss this in detail in the next section. By utilizing quench echo one can even find a uniformly adiabatic quench protocol for a given Hamiltonian by repeating the above process with different quench time scales.

# III. A CASE STUDY: ISING CHAIN IN A TRANSVERSE MAGNETIC FIELD

We now use a simple model to demonstrate our central ideas: Consider the quench dynamics of an Ising model in an transverse magnetic field [14]. The time-dependent Hamiltonian is

$$H(t) = -J \sum_{i=1}^{N} \left[ \sigma_i^x \sigma_{i+1}^x + g(t) \sigma_i^z \right],$$
 (3)

where J indicates the energy scale;  $\sigma_i^{\alpha}$ ,  $\alpha=x,y,z$  is the Pauli matrix on the i th lattice site; and g(t) is the reduced strength of the magnetic field, which varies with time. It is known that for this model there is a finite energy gap  $\Delta=2J\frac{\pi}{N}$  at  $g=\cos(\pi/N)$  when the size of the system N is finite. For simplicity, we consider a linear quench protocol

$$g(t) = \begin{cases} g_0 - \frac{t}{\tau_Q}, (0 < t < (g_0 - g_T)\tau_Q), \\ 2g_T - g_0 + \frac{t}{\tau_Q}, ((g_0 - g_T)\tau_Q < t < 2(g_0 - g_T)\tau_Q), \end{cases}$$
(4)

where  $\tau_Q$  is the time scale of the quench. The larger the  $\tau_Q$ , the slower the quench. In the forward quench the strength of the magnetic field is ramped from  $g=g_0$  to  $g=g_T$  continuously, and in the quench echo, it is ramped back from  $g=g_T$  to  $g=g_0$ , where  $g_T$  is the turnaround point. Initially the system is prepared in the ground state of  $H(g=g_0)$ . When one quenches the system at different rates (by choosing different  $\tau_Q$ ), the fidelity (2) will be different.

The Hamiltonian of the Ising model (3) can be decoupled into N independent fermionic modes [14].

$$H(t) = \sum_{k} \Lambda_{k}(g(t)) \left[ \left| +(t) \right\rangle_{k} \left\langle +(t) \right|_{k} - \left| -(t) \right\rangle_{k} \left\langle -(t) \right|_{k} \right], \tag{5}$$

where  $|+(t)\rangle_k$  and  $|-(t)\rangle_k$  are the two instantaneous eigenstates of the k mode. Their corresponding eigenenergies are  $\pm \Lambda_k(g(t))$ , and  $\Lambda(g(t)) = J\sqrt{g(t)^2 - 2g(t)\cos k + 1}$ . Here  $k = (2s+1)\pi/N$ ,  $s = 0,1,2,\cdots,N/2-1$  is the wave vector, and the number of spins N is even.

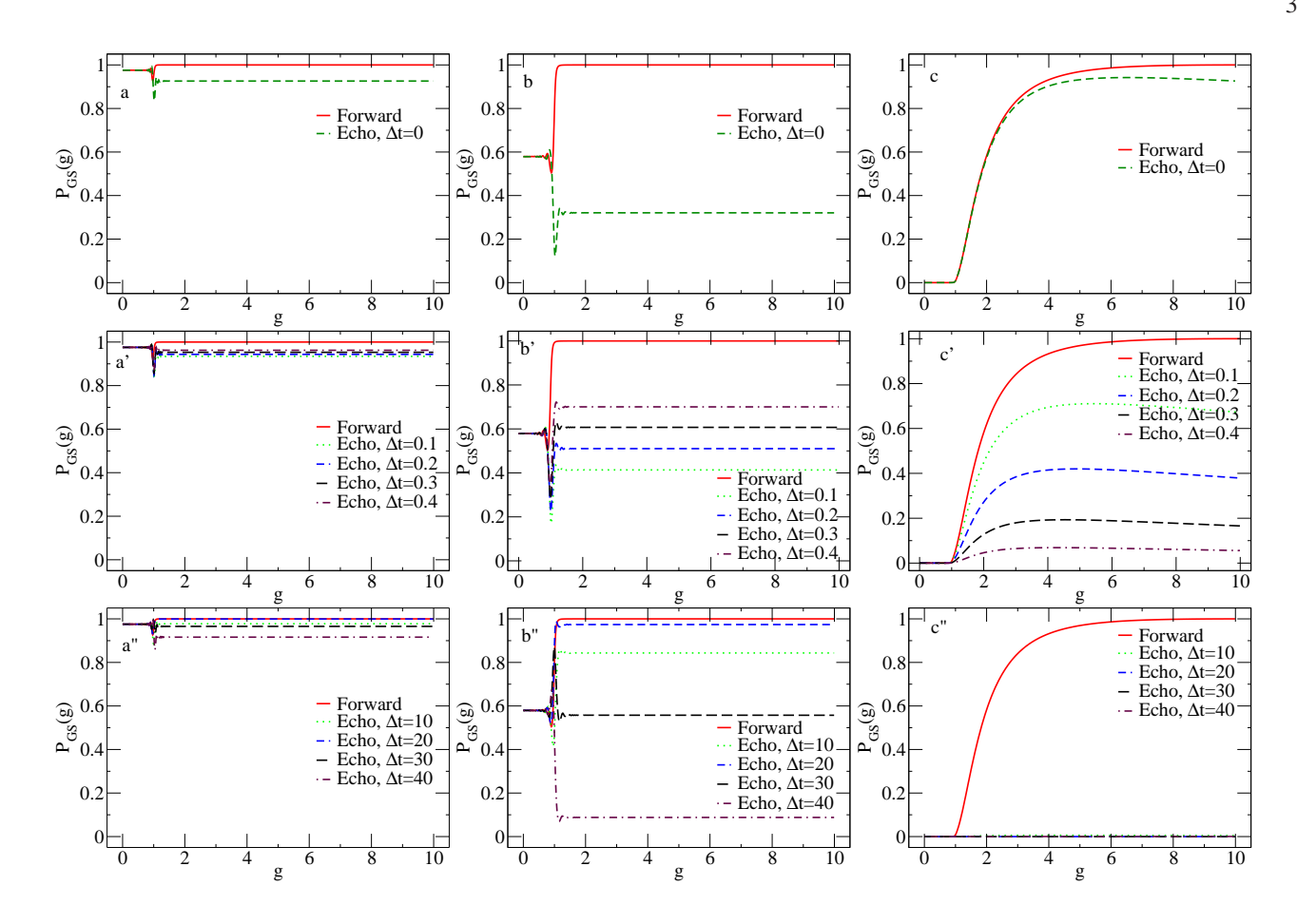


FIG. 1: Three regimes of the quench dynamics: (a) nearly adiabatic regime,  $\tau_Q=150$ ; (b) the intermediate regime  $\tau_Q=35$ ; and (c) nearly impulse regime  $\tau_Q=0.004$ . The horizontal axis represents the parameter g(t), which varies between 0 and 10, and the vertical axis represents the probability of the system being in the instantaneous ground state during the evolution. There is a quantum phase transition at  $g_c=1$ . The red solid line represents the forward quench (from  $g_0=10$  to  $g_T=0$ ) and the green dashed line represents the quench echo (from  $g_T=0$  to  $g_0=10$ ). In both the nearly adiabatic and the nearly impulse regimes, the fidelity at final moment is close to unity. In the first row (a)-(c), there is no time delay at the turnaround point. In the second row (a')-(c'), the delay time at  $g_T=0$  is  $\Delta t=0.1, 0.2, 0.3, 0.4$ . In the third row (a")-(c"), the delay time at  $g_T=0$  is  $\Delta t=0.1, 0.2, 0.3, 0.4$ . In the third row (a")-(c"), the delay time at  $g_T=0$  is  $g_T=0$  in the third row (a")-(c"), the delay time at  $g_T=0$  is  $g_T=0$  is g

We write the Schrödinger equation  $i\hbar \frac{\partial}{\partial t} |\Phi(t)\rangle = H(t) |\Phi(t)\rangle$  in the instantaneous eigenbases  $|+(t)\rangle_k$  and  $|-(t)\rangle_k$  of H(t), where  $|\Phi(t)\rangle = \prod_k \alpha_k(t) |+(t)\rangle_k + \beta_k(t) |-(t)\rangle_k$ . For simplicity we choose  $\hbar=1$  hereafter. For both the forward quench  $(0 < t < (g_0 - g_T)\tau_Q)$  and the backward  $((g_0 - g_T)\tau_Q < t < 2(g_0 - g_T)\tau_Q)$  process , the Schrödinger equation can be written as

$$i\frac{d}{dt} \begin{bmatrix} \alpha_k(t) \\ \beta_k(t) \end{bmatrix} = \begin{bmatrix} 2\Lambda_k(g(t)), \frac{-iJ^3 \sin k}{2\Lambda_k^2(g(t))} \frac{dg(t)}{dt} \\ \frac{iJ^3 \sin k}{2\Lambda_k^2(g(t))} \frac{dg(t)}{dt}, -2\Lambda_k(g(t)) \end{bmatrix} \begin{bmatrix} \alpha_k(t) \\ \beta_k(t) \end{bmatrix}, \tag{6}$$

where the initial condition for Eq. (6) is  $\alpha_k(t=0) = 0$ ,  $\beta_k(t=0) = 1$ . The modulus square of the overlap between the final state of Eq. (6) and the instantaneous ground state at  $g = g_0$  gives the fidelity (2)

$$F = P_{GS}(2(g_0 - g_T)\tau_Q) = \prod_{k>0} |\beta_k(2(g_0 - g_T)\tau_Q)|^2.$$
(7)

In the following, we will focus on the solution of the Eq. (7). We will consider both the numerical and the analytical results.

# A. Kibble-Zurek mechanism and three regimes

Before the quantitative study of the fidelity and its relation with the time scales of the quench, we describe the Kibble-Zurek mechanism (KZM) [15, 16] of second-order phase transitions, which provides a quantitative understanding of the quench process. The KZM describes e.g., the relation between the density of topological defects, which are generated during quenching across a phase transition, and the time scale of the quench (see Ref. [18] for a good review). The KZM was first introduced in the classical phase transitions [15, 16], and later generalized to quantum phase transitions [21]. In our study, however, we will not focus on the density of topological defects, but on the adiabaticity of the evolution of the system.

A quantum phase transition is characterized by a vanishing excitation gap  $\Delta(g(t)) \approx \Delta_0 |g(t) - g_c|^{z\nu}$  and a divergent correlation length  $\xi \approx \xi_0/|g(t) - g_c|^{\nu}$ , where z and  $\nu$  are the critical exponents, and  $\Delta_0$  and  $\xi_0$  are constants [14]. We define a dimensionless distance from the critical point  $g_c$  by

$$\epsilon(t) = \frac{g(t) - g_c}{g_c}. (8)$$

A generic  $\epsilon(t)$  can be linearized near the critical point  $\epsilon(t)=0$  as [17]:

$$\epsilon(t) \approx -\frac{t}{\tau_Q}.$$
 (9)

There are two interlinked time scales during a quench: the system reaction time given by the inverse of the gap  $\tau(\epsilon(t)) = 1/\Delta_0|g(t)-g_c|^{z\nu}$  and the time scale of transition given by  $|g(t)-g_c|^{z\nu}/\frac{d}{dt}|g(t)-g_c|^{z\nu}$ . Away from the critical point the reaction time is small in comparison with the time scale of transition and the evolution is adiabatic. Near the critical point, however, the opposite situation occurs and the evolution is approximately impulse (the state of the system is frozen out). The boundary  $\hat{t}$  between the two regions is determined by the relation  $\tau(\epsilon(t)) = \epsilon/\dot{\epsilon}|_{\hat{t}}$ , or

$$\frac{1}{|g(\hat{t}) - g_c|^{z\nu}} \sim \frac{|g(\hat{t}) - g_c|^{z\nu}}{\frac{d}{dt}|g(\hat{t}) - g_c|^{z\nu}}.$$
(10)

That is,  $\hat{t} \sim (\frac{\tau_Q}{\hat{t}})^{z\nu}$ , which gives  $\hat{t} \sim \tau_Q^{\frac{z\nu}{1+z\nu}}$  [16, 21]. For the Ising model, we have  $z=\nu=1$  resulting in  $\hat{t} \sim \tau_Q^{\frac{1}{2}}$  [21]. According to KZM when  $t \in (-\hat{t},\hat{t})$ , the system will not evolve (the wavefunction will be frozen). Outside this time interval the system will evolve approximately adiabatically.

For an infinitely large system, the energy gap is vanishingly small at the critical point, and one can always find a  $\hat{t}$ . According to the KZM this implies that, no matter how slow one quenches the Hamiltonian in an infinite system, the evolution across the critical point can never be adiabatic. For a finite-size system, however, there is a finite energy gap even at the critical point. When one quenches the system sufficiently slowly (large  $\tau_Q$ ),  $\hat{t}$  approaches very near the critical point where – for a finite systems – scalings no longer hold. As a consequence, the KZM does not lead to simple scaling, as  $\tau(\epsilon(t)) = \epsilon/\dot{\epsilon}|_{\hat{t}}$  leads to a more difficult equation which has to be solved to obtain  $\hat{t}$ . [22]. Indeed – in accord with the adiabatic theorem – the KZM predicts that when  $\tau_Q$  is larger than the inverse of the gap the transition will remain adiabatic throughout. Thus, a finite energy gap allows an adiabatic evolution across the critical point when the Hamiltonian is driven sufficiently slowly. This is the *adiabatic quench regime*. By contrast, when one quenches the Hamiltonian very fast (small  $\tau_Q$ ), there is a big  $\hat{t}$  and there is an approximately impulse regime for  $t \in (-\hat{t}, \hat{t})$  when the quench is essentially instantaneous. In this time interval the system will approximately cease to evolve – its wavefunction will be frozen. This is the so-called *impulse regime* [21, 23]. When one chooses a time scale of quench  $\tau_Q$  between the above two limiting cases, the system will evolve adiabatically when either  $t < -\hat{t}$  or  $t > \hat{t}$ , and will be frozen when  $\tau_Q$  is large enough, the evolution will be adiabatic; When  $\tau_Q$  is extremely small, the state of the system will be frozen; When  $\tau_Q$  is large enough, the evolution will be adiabatic; When  $\tau_Q$  is extremely small, the state of the system will be frozen; When  $\tau_Q$  is in between these two limiting cases, the process is in the intermediate regime.

## B. Numerical and analytical results

Having obtained the qualitative understanding of the quench dynamics from the above KZM arguments, in the following we will study the Ising model quantitatively, and compare the results with the estimates obtained above. We consider a spin chain with a finite size N=50, and start evolving it at  $g_0=10$  and let it turn around at  $g_T=0$ . There is a finite energy gap for this system at the quantum critical point  $g_c=1$ . We choose three different quench time scales  $\tau_Q=150$ ,  $\tau_Q=35$ , and  $\tau_Q=0.004$  which correspond to the adiabatic, intermediate, and impulse regimes. The system evolves under the time-dependent Schrödinger equation. We plot the probability  $P_{GS}(g)$  in the instantaneous ground state as a function of the controlling parameter g during the quench process in Fig. 1a-1c.

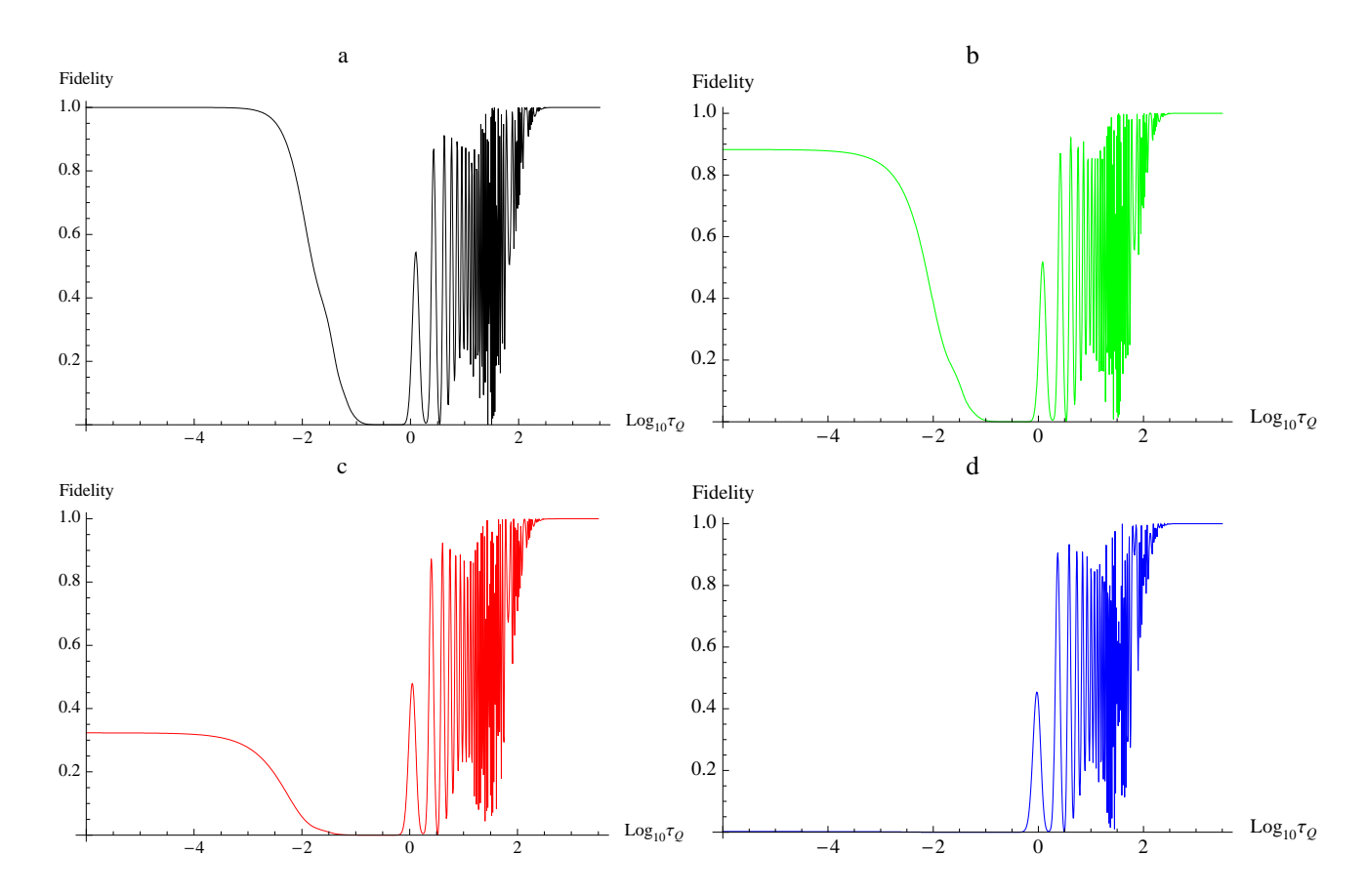


FIG. 2: The fidelity as a function of the time scale of quench  $\tau_Q$ . Panels (a)-(d) represent different free evolution time at turnaround point  $g_T=0$  before the quench echo. Here N=50, and start point at  $g_0=10$ , and the times of free evolutions are chosen to be  $\Delta t=0$ ,  $\Delta t=0.1$ ,  $\Delta t=0.3$ ,  $\Delta t=0.7$ . It can be seen that in the adiabatic regime the fidelity is always equal to unity, but in the impulse regime it is less than unity and varies with the time of free evolution  $\Delta t$ .

From Fig. 1a it can be seen that when the time scale of the quench is relatively large, the system evolves almost adiabatically in the whole range of the parameter  $g_T = 0 < g < g_0 = 10$ ,  $P_{GS}(g)$  is always close to unity (except a tiny decay and partial revival at the critical points. So is the fidelity of the quench echo (see Fig. 1a).

When the time scale of the quench is reduced to  $\tau_Q=35$  (see Fig. 1b), the quench dynamics enters the intermediate regime. It can be seen that away from the critical point, the evolution is adiabatic. But near the critical point, the probability in the instantaneous ground state  $P_{GS}(g)$  decays sharply and oscillates rapidly. This is due to the interstate transitions at the anti-cross point. Soon after passing through the quantum critical point the adiabatic evolution resumes.

When the time scale of the quench is further reduced to  $\tau_Q=0.004$  (almost instantaneous quench), the wave function of the system is nearly frozen. Hence, the probability of being in the instantaneous ground state is simply equal to the overlap of the initial state and the instantaneous ground state. In the backward quench, the same situation arises. Because in both the forward and the backward quench, the wave functions of the system are frozen, and hence are almost identical, the curves of  $P_{GS}(g)$  of the forward and the backward quench almost collapse onto the same curve (see Fig. 1c), and the fidelity at  $t=2(g_0-g_T)\tau_Q$  is close to unity.

We also plot the fidelity as a function of the quench time scale  $\tau_Q$  (see Fig. 2a). It can be seen that in both the impulse regime  $(\tau_Q < \sim 10^{-3})$  and the adiabatic regime  $(\tau_Q > \sim 10^{2.5})$ , the fidelity is equal to unity. This agrees with our intuition. Meanwhile, in the intermediate regime,  $\sim 10^{-3} < \tau_Q < \sim 10^{2.5}$ , the fidelity oscillates rapidly (see Fig. 2a). When we plot the fidelity as a function of the quench time  $\tau_Q$ , instead of  $\ln \tau_Q$ , we found that there is a regular quasi-periodic oscillation (see Fig. 3). We obtain an accurate expression of fidelity in the intermediate regime,

$$F \approx \prod_{k>0}^{\pi/2} \left| e^{-2\pi\tau_Q \sin^2 k} e^{i\phi_k} + \frac{2\pi\tau_Q \sin^2 k}{\Gamma^2 (1 - i\tau_Q \sin^2 k)} e^{-\pi\tau_Q \sin^2 k} e^{-i\phi_k} \right|^2, \tag{11}$$

where  $\phi_k = 2\tau_Q[(-g_T + \cos k)^2 + \sin^2 k \ln \sqrt{4\tau_Q(-g_T + \cos k)^2}]$ , and  $\Gamma(1 - i\tau_Q \sin^2 k)$  is the Gamma function (see Appendix

A for details of the derivation). From Fig. 3 it can be seen that the analytical results agree with the numerical simulations, and that the fidelity oscillates quasi-periodically with the increase of  $\tau_Q$  as expected. This oscillation can actually also be observed in Fig. 1 (see Fig. 1b' and Fig. 1c').

Numerical simulations agree with the results obtained from the KZM very well, i.e., they account for three regimes that correspond to different  $\tau_Q$ . We are especially interested in the first regime – the adiabatic regime. From Fig. 1a and Fig. 1c, it can be seen that in both the adiabatic regime and the impulse regime, the fidelity is close to unity. In the next subsection, we will introduce a method to eliminate the "degeneracy" of the adiabatic regime and the impulse regime.

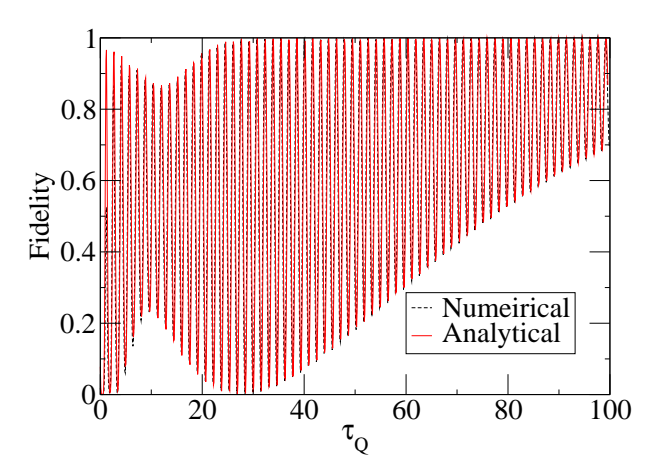


FIG. 3: Fidelity as a function of the time scale  $\tau_Q$ . Here the black dashed line represents the numerical results whereas the red solid line represents the analytical results (Eq. (11)). It can be seen that the analytical results (Eq. (11)) agree well with the numerical results except for the case  $\tau_Q \to 0$ , where the quench process enters the impulse regime. The length of the spin chain is N=50, and the delay time at the turnaround point is  $\Delta t=0$ .

# C. Free evolution and decay of fidelity

To distinguish the adiabatic and the impulse regime using quench echo, one can let the system evolve freely for some time at the turnaround point before quenching back. A study of the Landau-Zener problem with waiting at the minimum gap has been reported in Ref. [25]. It was observed that the waiting influences the excitation probability. Similarly in our study the free evolution at the turnaround point leads to a decay in the fidelity in the impulse regime, but makes no difference in the adiabatic regime (see Figs. 1a'-1c' and Figs. 1a''-1c''). The reason is straightforward. Let us first consider the adiabatic regime. Because the system is always in its instantaneous ground state, the effect of the free evolution is simply a global phase factor, which does not affect the fidelity (see Figs. 1a', 1a'', and Figs. 2b-2d). In the impulse regime, the wavefunction before the free evolution is the ground state of the initial Hamiltonian  $H(g_0 = 10)$ , and alternatively, a superposition of the excited and the ground states of  $H(g_T = 0)$ . The excited and ground states acquire different phase factors during the free evolution. Thus the wave function acquires relative phase factors in its components and is no longer the ground state of  $H(g_T = 0)$ , but a superposition of its ground and excited states. Hence, in the impulse regime when one quenches the system back to the initial Hamiltonian  $H(g_0 = 10)$ , the system will no longer be in its ground state, but in a superposition of the ground state and the excited states. As a result, the fidelity is less than unity (see Fig. 1c', Fig. 1c'', and Figs. 2b-2d). The length of time of the free evolution  $\Delta t$  also influences the fidelity. One can analytically calculate the fidelity as a function of the time of free evolution  $\Delta t$ :

$$|-(g=+\infty)\rangle_k = \sin\left[\frac{\theta_k}{2}\right]|+(g_T)\rangle_k + \cos\left[\frac{\theta_k}{2}\right]|-(g_T)\rangle_k$$

where  $\theta_k = \arctan(\frac{-\sin k}{\cos k - g_T})$ . After free evolution for  $\Delta t$ , the wave function becomes

$$\sin\left[\frac{\theta_k}{2}\right] e^{-i\Lambda_k(g_T)\Delta t} \left|+(g_T)\right\rangle_k + \cos\left[\frac{\theta_k}{2}\right] e^{i\Lambda_k(g_T)\Delta t} \left|-(g_T)\right\rangle_k.$$

The fidelity can then be calculated as

$$F = \prod_{k>0} \left( 1 - \frac{\sin^2 k \sin^2 \left[ \Lambda_k(g_T) \Delta t \right]}{1 - 2g_T \cos k + g_T^2} \right). \tag{12}$$

Note that for a fixed chain size, the value of  $\Delta t$  needed to scramble all the relevant phases is relevant to the range of the spectrum of the system or the size of gap  $\Lambda_k(g_T)$  of different k at the turnaround point  $g_T$ . When  $\Lambda_k(g_T)$  is very small, i.e., the energy spectrum of the system is concentrated within a very small energy range, one needs to wait for a long time in order to scramble all the relevant phases:  $\Delta t$  is inversely proportional to the energy scale J of  $\Lambda_k(g_T)$ . For a spin chain of N=50, when the time of free evolution is very short, e.g.,  $\Delta t=0.1$ , there is a pronounced decay in the fidelity in the impulse regime (see Fig. 2b). The analytical result gives  $F\approx 0.882$ , which agrees with the numerical result. The fidelity decreases with the increase of time of the free evolution. The fidelity decays to 0.002 when  $\Delta t=0.7$  (see Fig. 2d). Hence the quench echo with a free evolution at the turnaround point can distinguish the adiabatic and the impulse regime. Our numerical results confirm our theoretical predictions.

# IV. BEYOND THE LINEAR QUENCH

In the above discussion, we focused on the linear quench. One may repeat the above process with different  $\tau_Q$  until one finds the smallest  $\tau_Q^c$ , under which the process is sufficiently adiabatic, for example  $F \geq 0.9$ . Nevertheless, the linear quench with  $\tau_Q^c$  obtained above may waste a lot of time. The reason is obvious: in different regions of the parameter g, the energy gaps are different. According to KZM, different energy gaps correspond to different relaxation time  $\tau$ . For a linear quench protocol, we are treating the whole range of the parameter uniformly, and the relaxation time is determined by the global minimal energy gap. Thus, we waste a lot of time. Usually we want to ensure that the process not only nearly adiabatic but also as fast as possible. In the following we will consider nonlinear quench.

#### A. Adjusting quench rate to the instantaneous gap

An improved scheme is to divide the whole range of the parameter into many, e.g., M, parts with equal length  $(g_0-g_T)/M$ , and then apply the above linear quench protocol to these ranges separately to find the uniformly adiabatic quench for each range  $\tau_Q^{ci}$ ,  $i=1,2,\cdots,M$ . We can also use the KZM to find a uniformly adiabatic quench protocol. From the discussion in Section III.A we know that the transition time scale is given by the absolute value of  $\Delta(g(t))/\frac{d}{dt}\Delta(g(t))$ . Meanwhile, the relaxation time scale is given by  $1/\Delta(g(t))$ . When the former is many times larger than the latter, the process should be uniformly adiabatic. That is, when the parameter g(t) satisfies the relation

$$\left| \frac{\Delta(g(t))}{\frac{d}{dt}\Delta(g(t))} \right| = \frac{\gamma}{\Delta(g(t))}.$$
 (13)

where  $\gamma$  is a constant many times larger than unity, e.g.,  $\gamma = 10$ , the process is uniformly adiabatic in the sense that the ratio of two time scales remains a constant. Such a quench scheme is better than the linear quench. The solution to the above ordinary differential equation is

$$\Delta(g(t)) = \frac{1}{\mp \frac{1}{\gamma}t + c},\tag{14}$$

where  $\mp$  corresponds to the sign of  $\Delta/\dot{\Delta}$  on the left-hand-side of Eq. (13) being positive or negative, and c is a constant of integration. For simplicity c can be chosen such that at t=0  $\Delta$  in Eq. (14) is the minimal gap. Now, we know exactly the energy gap as a function of the controlling parameter (see Fig. 4a) [26]

$$\Delta(g(t)) = 2J\sqrt{1 - 2g(t)\cos(\frac{\pi}{N}) + g^2(t)}.$$
(15)

Therefore, c can be determined by  $g(t=0)=\cos(\pi/N)$ . Combining Eqs. (14) and (15), we find the following uniformly adiabatic quench protocol (see Fig. 4b)

$$g_{\rm KZ}(t) = \begin{cases} \cos(\frac{\pi}{N}) - \sqrt{-\left(\sin(\frac{\pi}{N})\right)^2 + \frac{(\gamma)^2}{4J^2 \left(t + \frac{\gamma}{2J\sin(\pi/N)}\right)^2}, \left(-\frac{\gamma}{2J\sin(\pi/N)} < t < 0\right) \\ \cos(\frac{\pi}{N}) + \sqrt{-\left(\sin(\frac{\pi}{N})\right)^2 + \frac{(\gamma)^2}{4J^2 \left(-t + \frac{\gamma}{2J\sin(\pi/N)}\right)^2}, \left(0 < t < \frac{\gamma}{2J\sin(\pi/N)}\right)} \end{cases}$$
(16)

It can be seen that the time required for the whole process (quenching the controlling parameter from g=0 to  $g=\infty$ ) is given by

$$\Delta t_{\rm KZ} = \frac{\gamma}{J\sin\left(\pi/N\right)} \approx \frac{\gamma N}{J\pi},$$
(17)

or  $\Delta t_{\rm KZ} = \frac{2\gamma}{\Delta_{\rm min}}$ , which is proportional to the chain size N and the ratio  $\gamma$ , and inversely proportional to the minimum energy gap  $\Delta_{\rm min} = 2J\sin\frac{\pi}{N} \approx 2J\frac{\pi}{N}$ . In linear quench the minimal time required for the adiabatic evolution grows with the system size like  $N^2$  [24]. The quench scheme of Eq. (16) is obviously better. This agrees with previous studies that "non-linear" quench can improve the adiabaticity (minimize excitation) [18–20]. The energy gap and the protocols for uniformly adiabatic quench (Eq. (16)) are shown in Fig. 4.

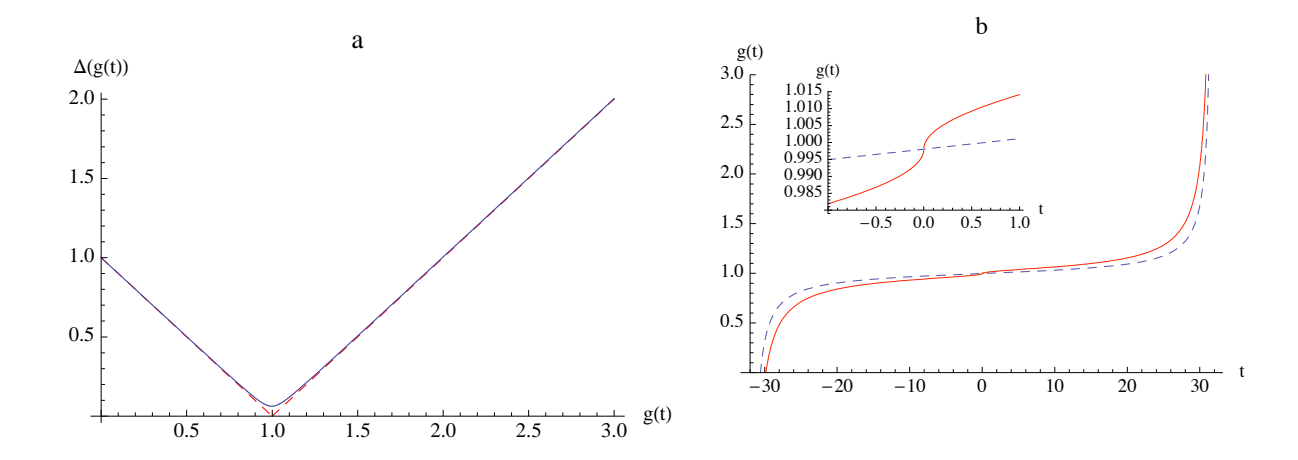


FIG. 4: (a) Energy gap as a function of the controlling parameter g for a finite size chain. Here the solid line indicates the spin chain of N=50 and the dashed line indicates the gap of an infinite chain. (b) The uniformly adiabatic quench protocol associated with the KZM criterion (solid) (16) and associated with RC criterion (dashed) (19). Here the ratio  $\gamma=2$ , and the energy scale J=1/2. We have chosen the condition  $g(t=0)=\cos{(\pi/N)}$ .

Note that the criterion for uniformly adiabatic evolution derived from the KZM (Eq. (13)) is similar, but not identical, to the criterion proposed by Roland and Cerf that was derived from the quantum adiabatic theorem (See Eq. (17) of reference [27]). In the RC model the energy gap is inversely proportional to  $\sqrt{N}$ , and the minimum time required is proportional to N. But in the Ising chain, the energy gap is inversely proportional to N, and the minimum time required is proportional to N. It can be proved that if one uses Roland and Cerf's criterion to evaluate the minimum time required for the uniformly adiabatic evolution, the minimum time is also proportional to N.

It is interesting to compare the two criteria for uniformly adiabatic evolution in the Ising chain. In the following we will first solve the equation of the quench protocol for uniformly adiabatic evolution  $g_{\rm RC}(t)$  associated with the Roland and Cerf's criterion and then simulate the dynamic evolution of the Ising chain with both  $g_{\rm RC}(t)$  and  $g_{\rm KZ}(t)$ . We will fix the time of quench process, and compare the fidelity of the two protocols. The Roland and Cerf's criterion (see Eq. (17) of Ref. [27]) is

$$\left| \frac{d}{dt} \left| g(t) - g_c \right| \right| = \frac{1}{\gamma'} \Delta^2(g(t)), \tag{18}$$

where  $\gamma'$  is the ratio between the two time scale. Obviously, when  $N \to \infty$ ,  $\Delta(g) = |g(t) - g_c|$  is valid for arbitrary g. In this respect, the two criteria, Eq. (13) and Eq. (18), are equivalent. Nevertheless, when N is finite, the two criteria differ slightly because the gap  $\Delta(g)$  deviates from  $|g(t) - g_c|$  near the critical point (see Eq. (15) and Fig. 4a). As a result there is a small discrepancy in the quench protocols  $g_{\rm RC}(t)$  and  $g_{\rm KZ}(t)$  associated with two criteria, especially when g(t) is close to  $g_c$ .

By substituting Eq. (15) into Eq. (18), we obtain the quench protocol:

$$g_{\rm RC}(t) = \cos(\frac{\pi}{N}) + \sin(\frac{\pi}{N}) \tan\left(\frac{2J\sin(\frac{\pi}{N})}{\gamma'}t\right), \left(-\frac{\gamma'N}{4J} < t < \frac{\gamma'N}{4J}\right). \tag{19}$$

We plot the solution  $g_{RC}(t)$  along with  $g_{KZ}(t)$  in Fig. 4b. There is a "kink" at the anti-cross point of the energy levels in  $g_{KZ}(t)$  associated with the KZM criterion, but there is none in  $g_{RC}(t)$  associated with the RC criterion (see Fig. 4b and the inset).

Although there is a singularity (divergent time derivative of g) in  $g_{\rm KZ}(t)$  at t=0, the time interval of this region is vanishingly small. As a result the total change in g in this singular region is very small (See Eq. 4b), and the eigenstates of H(t) do not change significantly within it. This is in the same spirit as quantum fidelity [30], where fidelity susceptibility diverges at quantum critical point, but the fidelity is nonzero indicating that the ground state does not changes significantly. Hence, the 'kink' at t=0 will not lead to a lot of excitations. Our simulation verifies this point. Similar to Eq. (17), we obtain the time required for the uniformly adiabatic evolution

$$\Delta t_{\rm RC} = \frac{\gamma' N}{2J}.\tag{20}$$

Comparing Eq. (17) and Eq. (20), we find that when  $\gamma' = \frac{2}{\pi}\gamma$ , the time required for two criteria are equal. In the following we will simulate the dynamics of the Ising chain under the two quench protocols: Eq. (16) and Eq. (19). Substituting Eq. (16) and Eq. (19) into Eq. (6), one obtains the instantaneous fidelity as a function of the time  $F = |\beta(t)|^2$  associated with two criteria. We plot the fidelity as a function of the time in Fig. 5. When one chooses a different initial condition, the fidelity as a function of the time differs a lot. In the left panel of Fig. 5, we plot the fidelity as a function of the time quenching from  $t = -\frac{\gamma}{2J\sin(\pi/N)}$  ( $g = -\infty$ ). The fidelity associated with the Roland and Cerf criterion decays when the system is near the anti-crossing point, and then revives. But the fidelity associated with the KZM does not change much, and remains close to unity all the time. At  $t = \frac{\gamma}{2J\sin(\pi/N)}$  ( $g = \infty$ ), the fidelity associated with the Roland and Cerf's criterion is a bit higher than that associated with the KZM. In the right panel of Fig. 5, we plot the fidelity as a function of the time starting from  $t = -\frac{1}{3}\frac{\gamma}{2J\sin(\pi/N)}$ . In this case the fidelity associated with the Roland and Cerf's criterion oscillates rapidly and finally reaches a stable value around 0.85. By contrast the fidelity associated with the KZM does not oscillate and remains very close to unity. From the above facts, we conclude that in some cases, the Roland and Cerf's criterion is better than the KZM criterion, but in some other cases, it is worse. Hence, we cannot say which criterion is definitely better, but the KZM provides new insights into the conditions for uniformly adiabatic evolution.

One is tempted at this point to undertake a variational study in search of optimal quenches. While such a study is beyond the scope of this paper, we note that in practical applications (e.g., adiabatic quantum computing) optimization would involve not just varying rate, but (as it was done in Fig. 5) also the starting and final points of the quenches can be brought closer to the "critical point". Resulting errors can be detected and the correct result can be ascertained by repeating the computation many times.

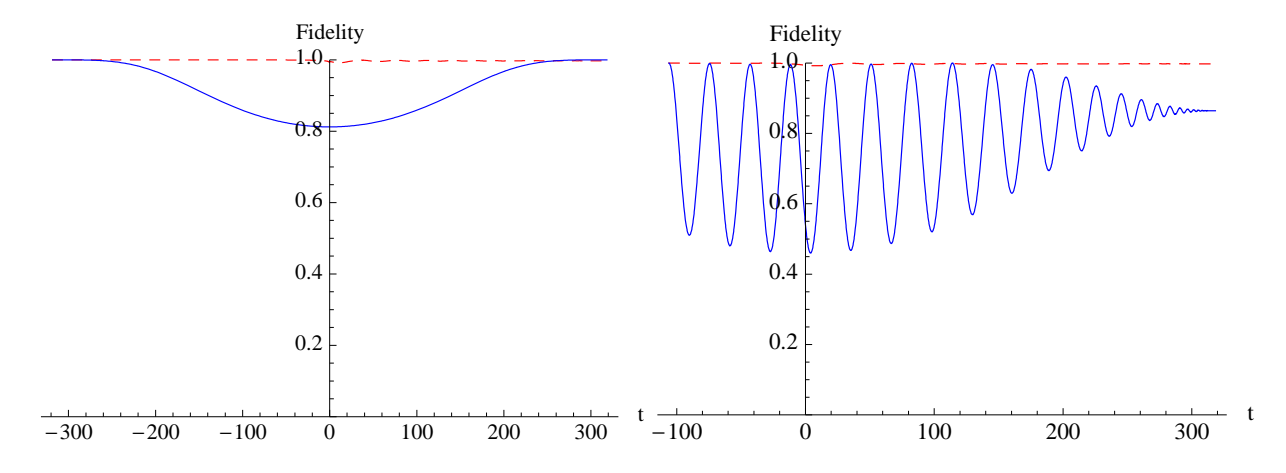


FIG. 5: Comparison of the Roland and Cerf criterion and the KZM criterion. The horizontal axis indicates the time, and the vertical axis depicts the instantaneous fidelity. The solid (dashed) line describes the fidelity as a function of the time t associated with the Roland and Cerf (KZM) criterion. Left panel: The evolution starts from the ground state of  $t=-\frac{\gamma N}{2J\pi}$  ( $g=-\infty$ ). Right panel: The evolution starts from the ground state of  $t=-\frac{1}{3}\frac{\gamma N}{2J\pi}$ .

#### B. Gauging the distance from the adiabatic quench

Fig. 2 indicates that when the time scale of the quench  $\tau_Q$  is in the range  $\tau_Q \in (10^{-1}, 1)$ , the fidelity is almost equal to zero. However, this does not reveal how far the quench is from the adiabaticity. For example when one out of many (N = 50 in our numerical simulation) modes get excited, the fidelity will decay to nearly zero due to the orthogonality of one mode. But, in a

sense, the system is still close to the ground state, as all but one excited state are empty. In this sense, the fidelity is not a good criterion for measuring how far away the quench is from the adiabatic evolution.

A better gauge of the distance of a quench process from the adiabaticity may be obtained using other variables, such as the magnetization per site along the direction of the external magnetic field

$$m = \frac{1}{N} \sum_{i=1}^{N} \langle \sigma_i^z \rangle = \frac{1}{N} \sum_{k=1}^{N} 2 \left| \beta_k ((g_0 - 2g_T) \tau_Q) \right|^2 - 1.$$
 (21)

When the magnetic field is large, the ground state corresponds to m=1. We plot the final magnetization as a function of  $\tau_Q$  in FIg. 6. In the range of  $\tau_Q \in (10^{-1},1)$ , the fidelity is vanishingly small, but the magnetization per site is still large. This indicates that the system is not very far away from the instantaneous ground state. Moreover, when one delays for some time at the turnaround point, the magnetization per site of the impulse regime will decrease, but that of the adiabatic regime will not (see Fig. 6). This is similar to the fidelity and agrees with our intuition. Last but not least, the magnetization is experimentally easier to the measure than the fidelity, and it has been used as a tool to study the adiabaticity of quantum dynamics in Ref. [29].

One can also use the kink density  $\frac{1}{2}\sum_i(1-\langle\sigma_i\sigma_{i+1}\rangle)$  [24] as a measure of the distance of the system from the adiabaticity. The relation between the fidelity and the density of defects has been studied in Ref. [31]. Other variables, such as the residual energy [32], can be also used to gauge the distance from the adiabatic quench. Such obvious measures of how far the quench is from the adiabaticity work well in the one-dimensional Ising model, but finding their useful analogues in other situations (e.g., adiabatic quantum computing) may not be easy.

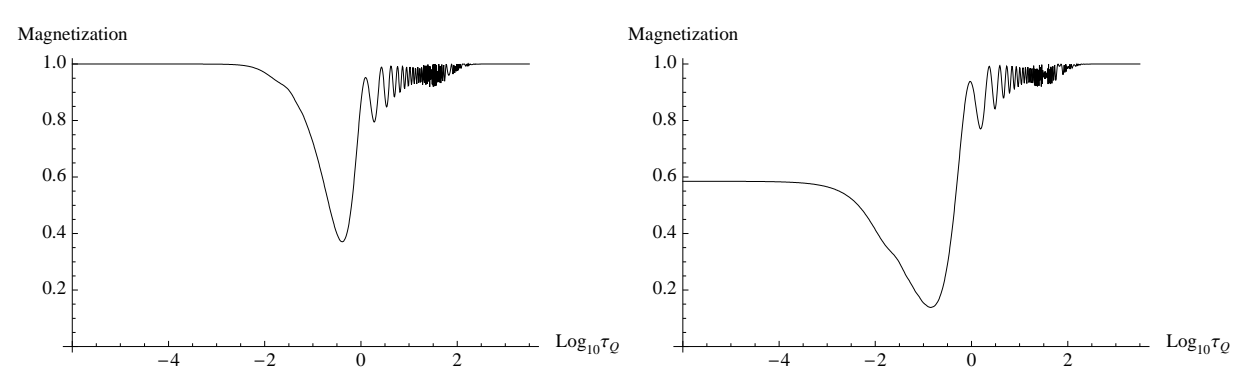


FIG. 6: Final magnetization of the Ising chain as a function of the time scale of the quench  $\tau_Q$ . All the parameters are the same as those in Fig. 2(a). One can see that the spin chain is not very far away from equilibrium except when the time scale of the quench is in the range  $\tau_Q \in (10^{-1}, 1)$ . Left panel: delay time  $\Delta t = 0$ ; Right panel: delay time  $\Delta t = 0.7$ .

# V. SUMMARY AND CONCLUSION

We have proposed a strategy to test the adiabaticity without knowing either the eigenstates or eigenenergies of the Hamiltonian. Instead of having to find the gap of the Hamiltonian, and then using the quantum adiabatic approximation to evaluate the adiabaticity, one can use a quench echo to evaluate the adiabaticity of an evolution. The underlying mechanism is that when the time scale of the quench is large in comparison with the inverse of the energy gap, both the forward and the backward evolutions are adiabatic. As a result, the fidelity of the initial state and the final state is close to unity. Otherwise, the evolution is not adiabatic, and the fidelity is less than unity. The method for testing the adiabaticity of an evolution presented in this paper is universally valid. It does not depend the model or the validity of conditions for adiabatic approximation. We further proposed a method for finding the uniformly adiabatic quench protocol based on the KZM, and discussed the problem of gauging how non-adiabatic is a quench. Given the importance of the adiabaticity in various applications, we believe that our results will be broadly applicable, and may be useful in experimental applications.

# Acknowledgments

This work is supported by U.S. Department of Energy through the LANL/LDRD Program. We thank Bogdan Damski, Anarb Das, and Rishi Sharma for helpful discussions.

# Appendix A: fidelity in the intermediate regime

From Refs. [24, 28], we know that in the wave vector *k* representation, the Schrödinger equation for the forward quench can be rewritten as Landau-Zener type equations (see Eq. (6) for a comparison):

$$i\frac{d}{dt'} \begin{bmatrix} v_k(t') \\ u_k(t') \end{bmatrix} = \frac{1}{2} \begin{bmatrix} \frac{t'}{\tau_Q'} & 1 \\ 1 & -\frac{t'}{\tau_Q'} \end{bmatrix} \begin{bmatrix} v_k(t') \\ u_k(t') \end{bmatrix}, \tag{A1}$$

where  $t'=4\tau_Q\sin k[-g(t)+\cos k]$  and  $\tau_Q'=4\tau_Q\sin^2 k$ . This equation can be solved in terms of Weber functions. The initial conditions are  $v_k(t'=-\infty)=0$  and  $u_k(t'=-\infty)=1$ . The solution for this equation is [28]

$$u_{k}(t) \approx e^{-\pi \tau_{Q} \sin^{2} k} e^{i\tau_{Q}[(-g+\cos k)^{2} + \sin^{2} k \ln \sqrt{4\tau_{Q}(-g+\cos k)^{2}}]},$$

$$v_{k}(t) \approx \frac{\sqrt{2\pi \tau_{Q} \sin^{2} k}}{\Gamma(1 - i\tau_{Q} \sin^{2} k)} e^{-\frac{\pi \tau_{Q} \sin^{2} k}{2}} e^{-i\tau_{Q}[(-g+\cos k)^{2} + \sin^{2} k \ln \sqrt{4\tau_{Q}(-g+\cos k)^{2}}]}.$$
(A2)

Similarly, we can obtain the solution for the quench echo. Combining the forward and the quench echo process, we find the solution of the fidelity (11). It is worth pointing out that the above solution is only good for the turnaround point far away from the critical point  $g_T \ll 1$ . For example  $g_T = 0.5$ .

- [1] A. Messiah Quantum Mechanics, (Dover Publications, Mineola, New York, 1999).
- [2] In recent years the conditions for the adiabatic approximation have become a subject of controversy [3, 29]. The standard criterion is found to be neither sufficient nor necessary [4]. Additional assumptions are required to ensure the stated conditions to be rigorous. See Ref. [5] for a clarification of weakness of adiabaticity conditions.
- [3] K.-P. Marzlin and B. C. Sanders, Phys. Rev. Lett. 93, 160408 (2004); D. M. Tong, K. Singh, L. C. Kwek, and C. H. Oh, Phys. Rev. Lett. 95, 110407 (2005); S. Boixo and R. D. Somma, Phys. Rev. A 81, 032308 (2010).
- [4] Jian-da Wu, Mei-sheng Zhao, Jian-lan Chen, Yong-de Zhang, Phys. Rev. A 77, 062114 (2008); Jiangfeng Du, Lingzhi Hu, Ya Wang, Jianda Wu, Meisheng Zhao, and Dieter Suter, Phys. Rev. Lett. 101, 060403 (2008).
- [5] S. N. Shevchenko, S. Ashhab, and Franco Nori, Physics Reports 492, 1 (2010).
- [6] E. Farhi, et al, Science, **292**, 472 (2001).
- [7] T. Kadowaki, and H. Nishimori, Phys. Rev. E 58, 5355 (1998).
- [8] A. Das, and B. K. Chakrabarti, Rev. Mod. Phys. 80, 1061 (2008).
- [9] Reference [10] studied the density of topological defects under such quench echo. But our emphasis is different.
- [10] V. Mukherjee, A. Dutta, and D. Sen, Phys. Rev. B 77, 214427 (2008); U. Divakaran and A. Dutta, Phys. Rev. B 79, 214408 (2009).
- [11] B. Damski, and W. H. Zurek, Phys. Rev. A 73, 063405 (2006).
- [12] P. Solinas, P. Ribeiro, and R. Mosseri, Phys. Rev. A 78, 052329 (2008).
- [13] S. Ashhab, J. R. Johansson, A. M. Zagoskin, and Franco Nori, Phys. Rev. A 75, 063414 (2008).
- [14] S. Sachdev Quantum Phase Transitions, (Cambridge University Press, Cambridge, 2000).
- [15] T. W. B. Kibble, J. Phys. A 9, 1387 (1976); Phys. Rep. 67, 183 (1980);
- [16] W. H. Zurek, Nature 317, 505 (1985); Acta Physica Polonica B 24, 1301 (1993); Phys. Rep. 276, 177 (1996).
- [17] Kibble-Zurek mechanism with nonlinear quench schemes is also discussed recently, see Refs. [18–20].
- [18] J. Dziarmaga, arXiv: 0912.4034, Adv. Phys. in press.
- [19] D. Sen, K. Sengupta, and S. Mondal, Phys. Rev. Lett. 101, 016806 (2008); Phys. Rev. B 79, 045128 (2009).
- [20] R. Barankov and A. Polkovnikov, Phys. Rev. Lett. 101, 076801 (2008).
- [21] W.H. Zurek, U. Dorner and P. Zoller, Phys. Rev. Lett. 95, 105701 (2005).
- [22] W. H. Zurek, L. M. A. Bettencourt, J. Dziarmaga, and N. D. Antunes, Acta. Phys. Polon. B 31, 2937 (2000).
- [23] B. Damski, Phys. Rev. Lett. 95, 035701 (2005); L. C. Wang, X. L. Huang, X. X. Yi, Eur. Phys. J. D 46, 345 (2008).
- [24] J. Dziarmaga, Phys. Rev. Lett. 95, 245701 (2005).
- [25] U. Divakaran, A. Dutta, and D. Sen, Phys. Rev. B 81, 054306 (2010).
- [26] The energy gap of other modes is much larger than the considered mode  $k = \pi/N$ . So one usually consider only the excitations (if there is any) in the smallest mode  $k = \pi/N$ , and ignore the excitations in the other modes
- [27] J. Roland and N. J. Cerf, Phys. Rev. A 65, 042308 (2002).
- [28] B. Damski, H. T. Quan, and W. H. Zurek, arXiv: 0911.5729.
- [29] A. Das arXiv: 0904.2172.
- [30] Paolo Zanardi, and Nikola Paunkovi, Phys. Rev. E 74, 031123 (2006).
- [31] L. Cincio, J.Dziarmaga, J. Meisner, and M. M. Rams, Phys. Rev. B 79, 094421 (2009).
- [32] F. Pellegrini, S. Montangero, G. E. Santoro, and R. Fazio, Phys. Rev. B 77, 140404 (2008).